Supporting Information

Photodynamic Therapy Mediated by Nontoxic Core-Shell Nanoparticles Synergize with Immune Checkpoint Blockade to Elicit Antitumor Immunity and Antimetastatic Effect on Breast Cancer

Xiaopin Duan,[†] Christina Chan,[†] Nining Guo,[†,‡] Wenbo Han,[†] Ralph R. Weichselbaum,[‡] and Wenbin Lin*[,†]

[†]Department of Chemistry, The University of Chicago, 929 E 57th Street, Chicago, IL 60637, USA

[‡]Department of Radiation and Cellular Oncology and The Ludwig Center for Metastasis Research, The University of Chicago, 5758 S Maryland Ave, Chicago, IL 60637, USA

E-mail: wenbinlin@uchicago.edu

Supporting Experimental Methods

Materials, Cell Lines, and Animals. All starting materials were purchased from Sigma-Aldrich and Fisher (USA), unless otherwise noted, and used without further purification. 1,2-dioleoyl-*sn*-glycero-3-phosphate (DOPA), 1,2-dioleyl-*sn*-glycero-3-phosphocholine (DOPC), cholesterol, and 1,2-distearoyl-*sn*-glycero-3-phosphoethanolamine-N-[amino(polyethylene glycol)2000] (DSPE-PEG2k) were purchased from Avanti Polar Lipids (USA). Pyrolipid was synthesized via esterification between 1-palmitoyl-2-hydroxy-*sn*-glycero-3-phosphocholine and pyropheophorbide-a as previously reported.[1]

Murine mammary carcinoma cells 4T1 and TUBO were purchased from the American Type Culture Collection (Rockville, MD, USA) and cultured in Dulbecco's Modified Eagle's Medium (DMEM) and RPMI-1640 medium (Gibco, Grand Island, NY, USA), respectively, supplemented with 10% fetal bovine serum, 100 U/mL penicillin G sodium and 100 μg/mL streptomycin sulfate in a humidified atmosphere containing 5% CO_2 at 37ºC.

BALB/c female mice (6 weeks, 18-22 g) were provided by Harlan Laboratories, Inc (USA). The study protocol was reviewed and approved by the Institutional Animal Care and Use Committee (IACUC) at the University of Chicago.

Synthesis of Zn-pyrophosphate (ZnP) Particles. Microemulsions were first formed by the addition of 0.2 mL $Na_4P_2O_7 \cdot 10H_2O$ (25 mg/mL in water) and 0.2 mL $Zn(NO_3)_2 \cdot 6H_2O$ (100 mg/mL

in water) to two separate surfactant system mixtures (5 mL, 0.3 M TritonX-100, 1.5 M hexanol in cyclohexane). The separate microemulsions were stirred vigorously for 15 min at room temperature. 40 μL of the DOPA solution (200 mg/mL in $CHCl_3$) was added to the $Na_4P_2O_7 \cdot 10H_2O$ solution, and the mixture was stirred 15 min, until a clear solution formed. Then, $Zn(NO_3)_2 \cdot 6H_2O$ solution was added slowly into $Na_4P_2O_7 \cdot 10H_2O$ solution, stirring, and the combined solution was allowed to react for 30 min at room temperature. Particles precipitated after adding 20 mL ethanol and obtained by centrifuging at 13,000 rpm for 30 min. The resulting pellet was washed once with 50% EtOH/cyclohexane and twice with 50% EtOH/THF, then redispersed in THF. Particles were purified by filtration through a 200 nm syringe filter.

X-ray absorption spectroscopy

Data collection. X-ray absorption data were collected at Beamline 10-BM-A, B at the Advanced Photon Source (APS) at Argonne National Laboratory. Spectra were collected at the zinc K-edge (9659 eV) in transmission mode. The X-ray beam was monochromatized by a Si(111) monochromater and detuned by 50% to reduce the contribution of higher-order harmonics below the level of noise. A metallic zinc foil standard was used as a reference for energy calibration and was measured simultaneously with experimental samples. The incident beam intensity (I_0), transmitted beam intensity (I_t), and reference (I_r) were measured by 20 cm ionization chambers with gas compositions of 99% N_2 and 1% Ar, 45% N_2 and 55% Ar, and 100% N_2, respectivelyData were collected over six regions: -250 to -30 eV (10 eV step size, dwell time of 0.25 s), -30 to -12 eV (5 eV step size, dwell time of 0.5 s), -12 to 30 eV (0.5 eV step size, dwell time of 1 s), 30 eV to 6 $Å^{-1}$, (0.05 $Å^{-1}$ step size, dwell time of 2 s), 6 $Å^{-1}$ to 12 $Å^{-1}$, (0.05 $Å^{-1}$ step size, dwell time of 4 s), 12 $Å^{-1}$ to 15 $Å^{-1}$, (0.05 $Å^{-1}$ step size, dwell time of 8 s). Multiple X-ray absorption spectra were collected at room temperature for each sample. Samples were ground and mixed with polyethyleneglycol (PEG) and packed in a 6-shooter sample holder to achieve adequate absorption length.

Data processing. Data were processed using the Athena and Artemis programs of the IFEFFIT package based on FEFF 6.[2,3] Prior to merging, spectra were calibrated against the reference spectra and aligned to the first peak in the smoothed first derivative of the absorption spectrum, the

background noise was removed, and the spectra were processed to obtain a normalized unit edge step.

EXAFS fitting. Fits of the EXAFS regions were performed using the Artemis program of the IFEFFIT package. Fits were performed with a *k*-weight of 3 in *R*-space. Refinement was performed by optimizing an amplitude factor S_0^2 and energy shift ΔE_0, which are common to all paths, in addition to parameters for bond length (ΔR) and Debye-Waller factor (σ^2). Due to the complexity of coordination environment of the ZnP@pyro, only first and second shells were included into EXAFS fitting. The scatting paths used for the fitting were generated from crystal structure GUQTOB, obtained from Cambridge Structural Database. We proposed that Zn can coordinate with phosphate bidentately or monodentately. A parameter (Fract) was introduced to estimate the percentage of both environments. The EXAFS fitting indicates the first shell is composed with 4 oxygen, with Zn-O distance of 1.965 ± 0.028. The second shell is composed with 0.48 ± 0.36 phosphine (bidentate), with Zn-P distance of 2.896 ± 0.080; as well as 3.04 ± 0.72 phosphine (monodentate), with Zn-P distance of 3.129 ± 0.019.

Preparation and Characterization of ZnP@pyro. ZnP@pyro was prepared by adding a THF solution (80 μL) of DOPC, cholesterol, pyrolipid, and DSPE-PEG2k (2:1:1:1 in molar ratio) and ZnP particles to 500 μL of 30% (v/v) ethanol/water at 60 °C. The mixture was stirred at 1,700 rpm for 1 min. THF and ethanol were completely evaporated and the ZnP@pyro solution was allowed to cool down to room temperature. The particle size and zeta potential of ZnP@pyro were determined by dynamic light scattering (DLS) using a Zetasizer (Nano ZS, Malvern, UK). Transmission electron microscopy (TEM, Tecnai Spirit, FEI, USA) was used to observe the morphology of ZnP@pyro. To determine pyrolipid loading, ZnP@pyro was centrifuged at 13,000 rpm for 30 min, the supernatant was removed and the particles were resuspended in THF which dissolves the lipid layer to release pyrolipid. The amount of pyrolipid in the nanoparticle suspension was then determined by the absorption at 669 nm using a UV-vis spectrophotometer (UV-2401PC, Shimadzu, Japan). The colloidal stability of ZnP@pyro was evaluated in the presence of bovine serum albumin (BSA). Briefly, ZnP@pyro diluted in phosphate buffered solution (PBS) containing 5 mg/mL BSA was incubated at 37ºC, and the change of particle size and PDI over time was determined by DLS.

Fluorescence Quenching. The fluorescence of ZnP@pyro with intact or disrupted lipid layer was measured to calculate the fluorescence quenching efficiency. ZnP@pyro was diluted in PBS as intact sample or in PBS containing 0.5% Triton X-100 to disrupt the lipid layer. The samples were subjected to spectrofluorophotometer (RF-5301PC, Shimadzu, Japan) to measure fluorescence spectra (λex = 427 nm, λem = 600-750 nm). The fluorescence intensity at 675 nm for ZnP@pyro with an intact lipid layer was normalized to ZnP@pyro with a disrupted lipid layer to calculate the quenching efficiency.

Singlet Oxygen Generation. The singlet oxygen sensor green (SOSG) reagent (Life Technologies, USA) was employed for the detection of singlet oxygen generated by ZnP@pyro upon irradiation. After lipid coating, ZnP@pyro was centrifuged at 13,000 rpm for 30 min. The supernatant containing free pyrolipid, liposome, and porphysome was discarded and the pellet was resuspended in PBS. 5 μL of freshly prepared SOSG solution in methanol (5 mM) was mixed with 2 mL of ZnP@pyro in PBS without or with 0.5% Triton X-100. Free pyrolipid at the same pyrolipid concentration as ZnP@pyro served as a control. Samples were treated with LED with a wavelength of 670 nm and energy irradiance of 120 mW/cm^2 for 10 s, 20 s, 30 s, 40 s, 50 s, 75 s, 100 s, and 250 s, and SOSG fluorescence was measured at an excitation at 504 nm and emission at 525 nm. There was no pyrolipid fluorescence contribution within this emission window.

Cellular Uptake and Efflux. 4T1 cells seeded in 6-well plates (5 × 10^4 cells per well) were incubated with ZnP@pyro or free pyrolipid at a pyrolipid concentration of 2 μM for 1, 2, 4, and 24 h. Cells were then collected, washed three times with PBS, counted with a hemocytometer, and lysed with 0.5% (w/v) sodium dodecyl sulfate (SDS, pH 8.0). The fluorescence intensity of pyrolipid was determined by fluorimetry (λex = 427 nm, λem = 675 nm) using a spectrofluorophotometer (RF-5301PC, Shimadzu, Japan). Uptake level was expressed as the amount of pyrolipid (pmol) per 10^5 cells.

To investigate the efflux of pyrolipid, 4T1 cells were incubated with ZnP@pyro or free pyrolipid at a pyrolipid dose of 2 μM for 4 h, the culture medium was then discarded and the cells were washed with PBS three times. 2 mL of fresh culture medium was added to each well and cells were further incubated for 1, 2, 4, and 24 h. After that, the culture medium was collected and subjected

to fluorimetry to determine the pyrolipid concentration for the quantification of pyrolipid efflux after adding 0.5% Triton X-100 to the medium. Results were expressed as the percent of the amount of pyrolipid being effluxed compared to the 4-h cellular uptake amount.

The internalization and intracellular distribution of pyrolipid was directly observed under CLSM. ZnP@pyro was incubated with 4T1 cells for 1 h, 2 h, 4 h, and 24 h, respectively. The cells were washed with PBS three times, fixed with 4% paraformaldehyde, and observed under CLSM (FV1000, Olympus, Japan) using a 405 nm laser.

Cytotoxicity Assay. 4T1 cells seeded in 96-well plates at a density of 2×10^3 cells per well were first incubated with ZnP@pyro or free pyrolipid at different pyrolipid concentrations for 24 h, irradiated with LED light (670 nm) at a light dose of 54 J/cm^2 and then incubated for another 48 h. Cell viability was detected by MTS assay (Promega, Madison, WI) according to the manufacturer's instructions. IC_{50} values were calculated from curves constructed by plotting cell viability (%) versus drug concentration (μM). All experiments were performed in triplicate.

Apoptosis Analysis in Vitro. 4T1 cells seeded in 6-well plates (5×10^4 cells/well) were treated with ZnP@pyro or free pyrolipid at a pyrolipid concentration of 0.2 μM for 24 h, irradiated with LED light (670 nm) at light dose of 54 J/cm^2 and then incubated for another 48 h. Treated cells were harvested, washed twice with ice-cold PBS, stained with Alexa Fluor 488-Annexin V and propidium iodide (PI) for 15 min at room temperature in the dark, and then analyzed by flow cytometry.

For CLSM imaging, 4T1 cells were seeded on 10 mm^2 glass coverslips placed in 6-well plates at a density of 5×10^4 cells per well and incubated with ZnP@pyro or free pyrolipid at a pyrolipid concentration of 0.2 μM for 24 h, irradiated with LED light (670 nm) at a light dose of 54 J/cm^2 and then incubated for another 48 h. After fixing with 4% paraformaldehyde, cells were stained with 10 μg/mL of DAPI and Alexa Fluor 488-Annexin V and then observed using CLSM at excitation wavelengths of 405 and 488 nm to visualize nuclei (blue fluorescence) and cell apoptosis (green fluorescence).

In Vitro Calreticulin Assay. CRT exposure induced by ZnP@pyro was evaluated by flow cytometry and immunofluorescence. For flow cytometry analysis, 4T1 cells were cultured with

ZnP@pyro or free pyrolipid at an equivalent pyrolipid dose of 0.2 μM for 24 h. Then, cells were irradiated with LED light (670 nm) at 60 mW/cm^2 for 15 min (equals to 54 J/cm^2). Following further incubation of 4 h, the cells were collected, incubated with Alexa Fluor 488-CRT antibody for 2 h, and stained with PI. The samples were analyzed by flow cytometer (LSRII Orange, BD, USA) to identify cell surface CRT. The fluorescence intensity of stained cells was gated on PI-negative cells. For immunofluorescence analysis, treated cells were washed with PBS three times, incubated with Alexa Fluor 488-CRT antibody for 2 h, stained with DAPI, and observed under CLSM using 405 nm and 488 nm lasers for visualizing nuclei and CRT expression on the cell membrane, respectively.

Apoptosis, Calreticulin Exposure and Cytokines Release in Vivo. The 4T1 tumor model was generated by an orthotopic injection of 5 ×10^4 cells into the mammary fat pads of the mice and tumors were allowed to grow until ~100 mm^3 before experiments. Tumor-bearing mice were intravenously (i.v.) injected with ZnP@pyro or free pyrolipid at a pyrolipid dose of 6 mg/kg on day 0. Twenty-four hours after injection (day 1), mice were anesthetized with 2% (v/v) isoflurane and tumors were irradiated with a 670 nm light-emitting diode (LED) at a light dose of 180 J/cm^2 given at 100 mW/cm^2. On day 3, tumors were excised, embedded in optimal cutting temperature (OCT) medium, sectioned into 5-μm slices, and subjected to hematoxylin and eosin (H&E) staining for histopathological analysis, or TdT-mediated dUTP nick end labeling (TUNEL, Invitrogen, USA) assay for quantifying the in vivo apoptosis, or CRT immunofluorescence staining for determining the CRT exposure on 4T1 tumors. At the same time, blood was collected on Days 0, 1, 2 and 3, and the serum IL-6, TNF-α and IFN-γ production was determined by enzyme-linked immunosorbent assay (ELISA, R&D Systems, USA) to evaluate the acute inflammation evoked by the treatment.

Pharmacokinetics and Biodistribution. The 4T1 tumor-bearing mice were intravenously administrated with ZnP@pyro at a pyrolipid dose of 6 mg/kg. Animals were sacrificed (n = 3) at 5 min, 1 h, 3 h, 8 h, 24 h, and 48 h after administration. After collecting the blood, liver, lung, spleen, kidney, bladder and tumor were harvested. Blood was immediately centrifuged at 3,000 rpm for 10 min to harvest plasma samples. Methanol was added to the plasma for deproteinization and extraction of the pyrolipid, followed by centrifugation at 10,000 rpm for 10 min. Organs and

tumors were homogenized in 1 mL methanol, followed by centrifugation at 10,000 rpm for 10 min. The content of pyrolipid in supernatant was then measured by fluorimetry. The tumors were also sectioned and observed under CLSM using a 405 nm laser to visualize the uptake of ZnP@pyro in tumors. The biodistribution of free pyrolipid at 24 h after intravenous injection was also investigated and compared with ZnP@pyro.

Antitumor and Antimetastatic Activity on Orthotopic 4T1 model. Mice bearing 4T1 tumors were randomly divided into four groups (n = 5): PBS; anti-PD-L1; ZnP@pyro with irradiation; ZnP@pyro with irradiation plus anti-PD-L1. ZnP@pyro was i.v. injected into animals at a pyrolipid dose of 6 mg/kg every two days for a total of three injections. Twenty-four hours after each injection, mice were anesthetized with 2% (v/v) isoflurane and tumors were irradiated with a 670 nm LED at a light dose of 180 J/cm^2 given at 100 mW/cm^2. After irradiation, mice were immediately intraperitoneally injected with PD-L1 antibody at a dose of 75 μg/mouse. Body weights and tumor volumes were monitored and recorded over a period of 23 days. The tumor size was measured with a digital caliper and calculated as follows: (width^2 × length)/2. At the end of experiment, mice were sacrificed, and tumors were excised, weighed and photographed. Lungs were also harvested, observed for the gross examination of tumor nodules, or sectioned and stained with H&E for quantification of metastasis area, or digested with collagenase type IV/elastase cocktail and cultured with 60 μM 6-thiogunine for 10 days. The colonies formed by clonogenic metastatic cancer cells were then fixed with methanol and stained with 0.1% crystal violet. For quantification, the crystal violet stained colonies were dissolved with 10% acetic acid and their absorbance at 590 nm was measured and normalized to the PBS control group.

Abscopal Effect on Bilateral 4T1 and TUBO Models. BALB/c mice were injected s.c. with 5 × 10^4 4T1 cells or 1 × 10^6 TUBO cells in the right flank (primary tumor) and 1 × 10^4 4T1 cells or 2 × 10^5 TUBO cells in the left flank (distant tumor). When the primary tumors reached ~100 mm^3, mice were randomly divided into four groups (n = 5): PBS; anti-PD-L1; ZnP@pyro with irradiation; ZnP@pyro with irradiation plus anti-PD-L1. ZnP@pyro was i.v. injected to animals at a pyrolipid dose of 6 mg/kg every two days for a total of three injections. Twenty four hours after injection, mice were anesthetized with 2% (v/v) isoflurane and primary tumors were irradiated with a 670 nm LED at a light dose of 180 J/cm^2 given at 100 mW/cm^2. After irradiation, mice were

i.p. injected immediately with PD-L1 antibody at a dose of 75 μg/mouse. The primary and secondary tumor size and body weight were monitored every day. All mice were sacrificed when the primary tumor size of control group exceeded 2 cm^3, and the excised tumors were weighed.

ELISPOT Assay. Tumor-specific immune responses to IFN-γ was measured *in vitro* by ELISPOT assay (Mouse IFN gamma ELISPOT Ready-SET-Go!®; Cat. No. 88-7384-88; eBioscience). A Millipore Multiscreen HTS-IP plate was coated overnight at 4 °C with anti-Mouse IFN-γ capture antibody. Single-cell suspensions of splenocytes were obtained from TUBO tumor-carrying mice and seeded onto the antibody-coated plate at a concentration of 2×10^5 cells/well. Cells were incubated with 3T3/KB cells or 3T3/NKB cells (2×10^4 cells/well) for 48 h at 37°C and then discarded. The plate was then incubated with biotin-conjugated anti-IFN-γ detection antibody at room temperature for 2 h, followed by incubation with Avidin-HRP for 2 h at room temperature. AEC substrate solution (Sigma, Cat. AEC101) was added for cytokine spot detection.

Flow Cytometry Assay for Immune Response. Tumors were harvested, treated with 1 mg/mL collagenase I (Gibco™, USA) for 1 h, and ground with the rubber end of a syringe. Cells were filtered through nylon mesh filters and washed with PBS. The single-cell suspension was incubated with anti-CD16/32 (clone 93; eBiosciences) to reduce nonspecific binding to FcRs. Cells were further stained with the following fluorochrome-conjugated antibodies: CD45 (30-F11), CD3e (145-2C11), CD4 (GK1.5), CD8 (53-6.7), B220 (RA3-6B2), NKp46 (29A1.4), CD25 (PC61.5), Foxp3 (FJK-16s), and PI staining solution (all from eBioscience). LSR FORTESSA (BD Biosciences) was used for cell acquisition, and data analysis was carried out using FlowJo software (TreeStar, Ashland, OR).

Supporting Figures

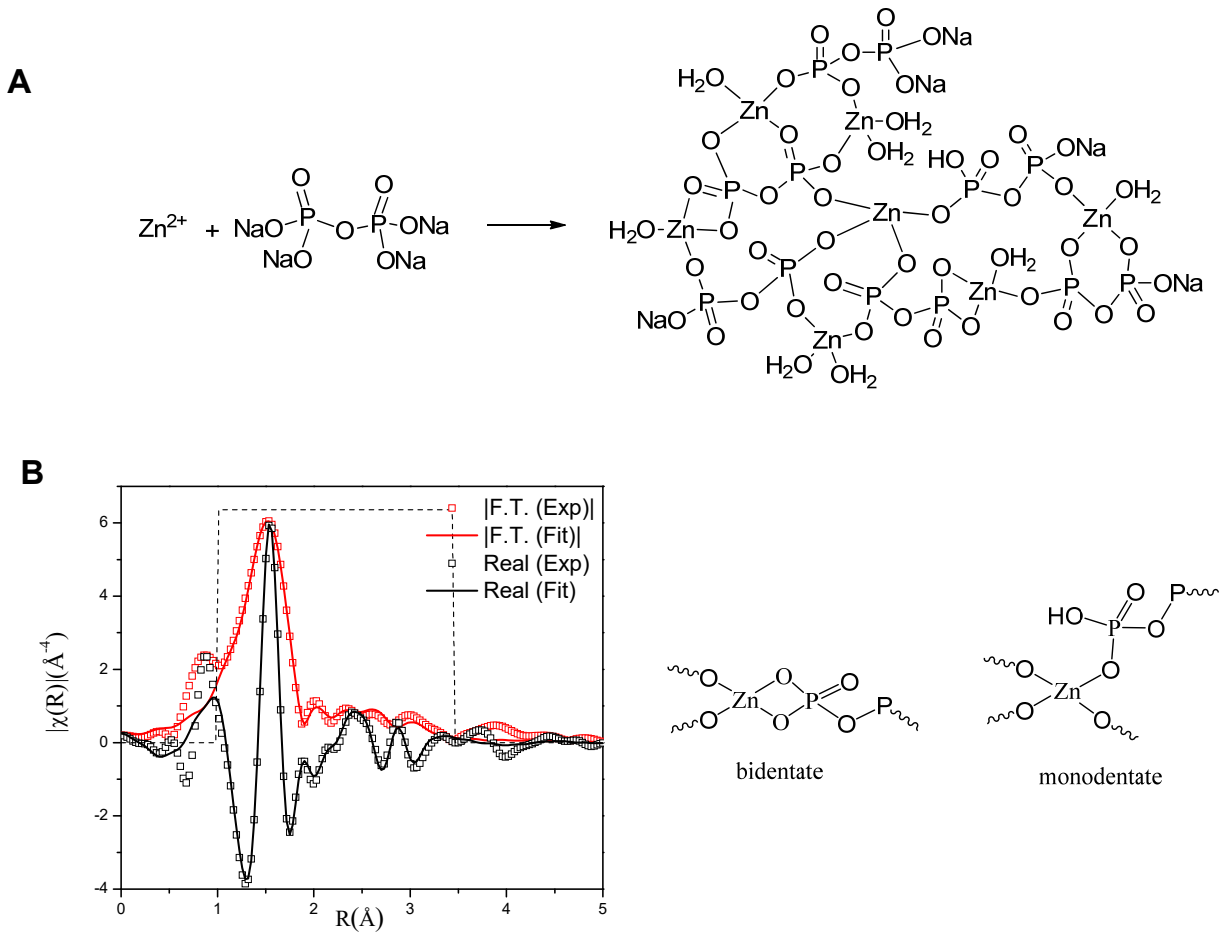

Figure S1. (A) Synthesis and proposed structure of ZnP particles. (B) Left, Experimental EXAFS spectra and fits of ZnP@pyro in R space showing the magnitude of Fourier Transform (red hollow squares, red solid line) and real components (hollow squares, dashed line). The fitting range was 1.0 – 3.45 Å in R space (within the dashed lines). Bottom shows the proposed ways of Zn coordinating to phosphate. Right, scheme showing bidentate (chelating) vs. monodentate phosphate coordination modes used in fitting the EXAFS data.

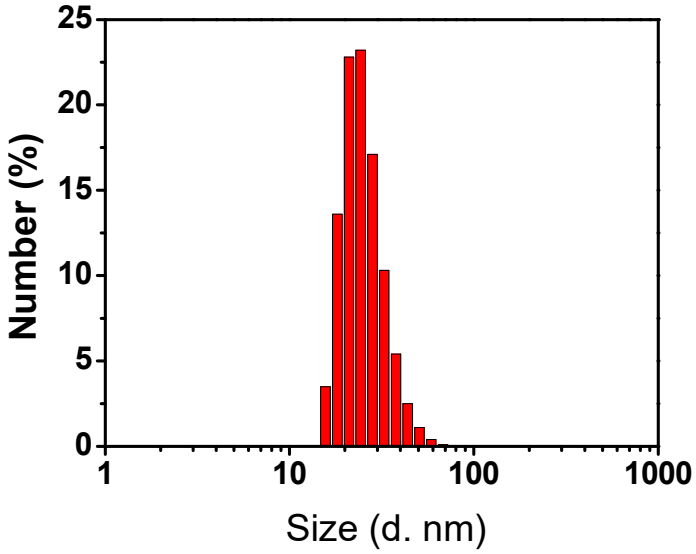

Figure S2. Number-average diameters of ZnP in THF, measured by DLS.

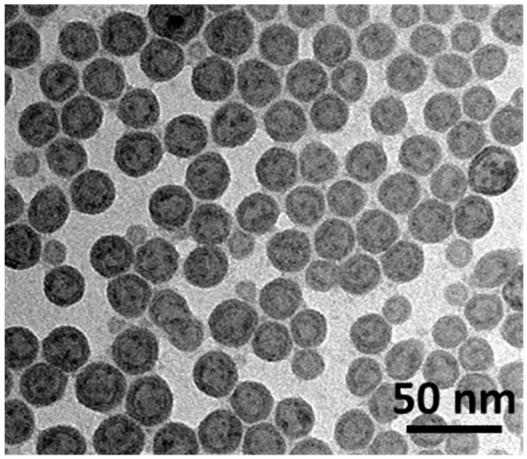

Figure S3. TEM image showing that ZnP was generally spherical in shape with good monodispersity.

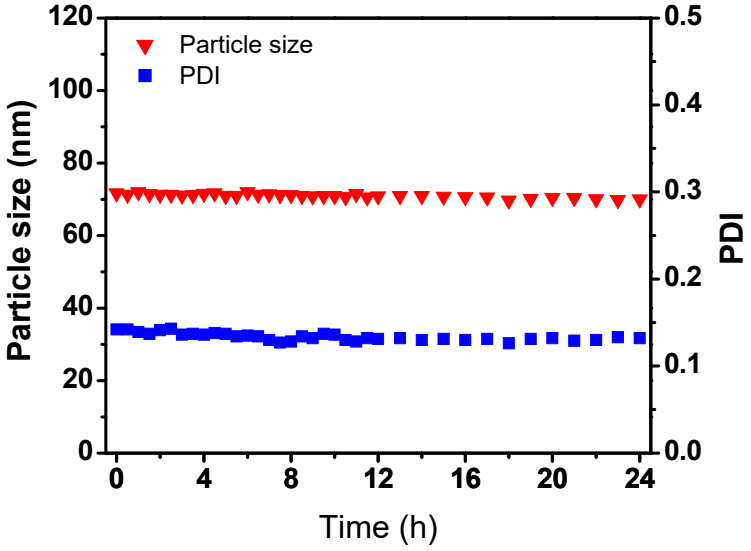

Figure S4. Time-dependent particle size and PDI changes of ZnP@pyro in PBS containing 5 mg/mL BSA at 37 °C.

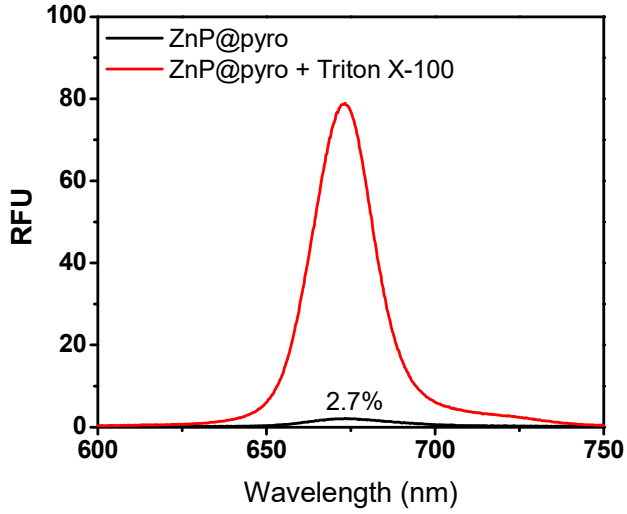

Figure S5. Fluorescence quenching of ZnP@pyro. Spectra were taken before and after addition of Triton X-100 to disrupt the lipid layer (excitation: 427 nm, emission: 600-750 nm).

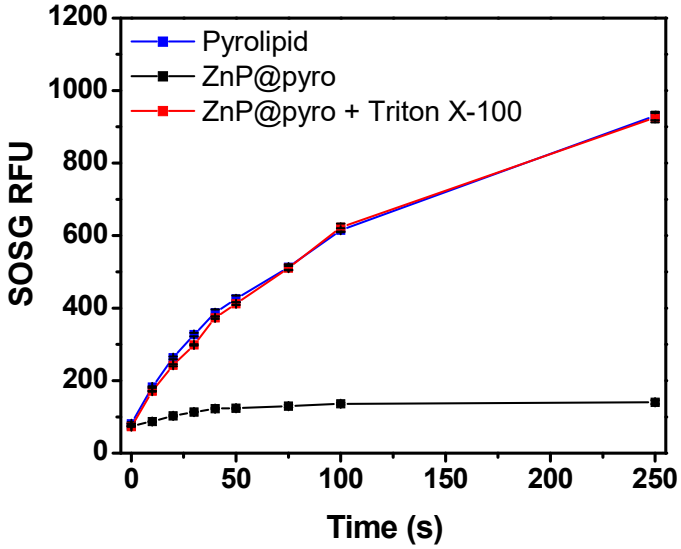

Figure S6. Singlet oxygen generation of ZnP@pyro with intact or disrupted lipid layer upon light irradiation (670 nm, 60 mW/cm^2), as determined by SOSG.

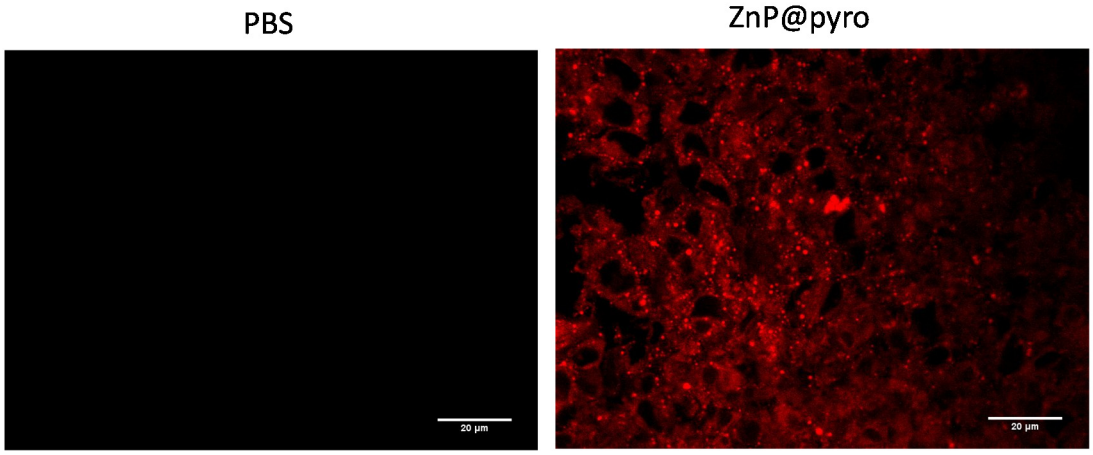

Figure S7. CLSM image showing the distribution of disassociated pyrolipid in the tumor 24 h after ZnP@pyro injection. A 405 nm laser was used to observe the fluorescence of pyrolipid (scale bar = 20 μm).

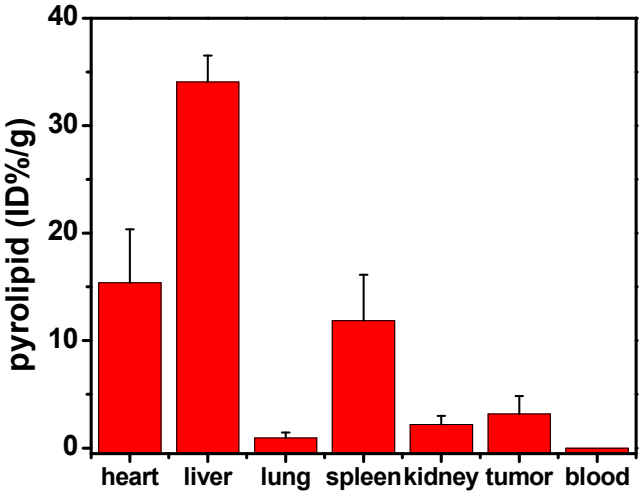

Figure S8. Biodistribution and tumor uptake of free pyrolipid in 4T1 tumor-bearing mice at 24 h after intravenous administration. Data are expressed as means ± s.d. (n = 3).

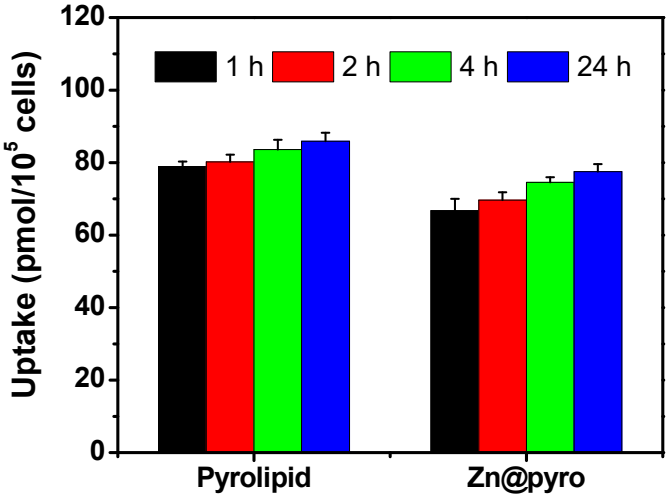

Figure S9. Time-dependent cellular uptake of free pyrolipid and ZnP@pyro in 4T1 cells.

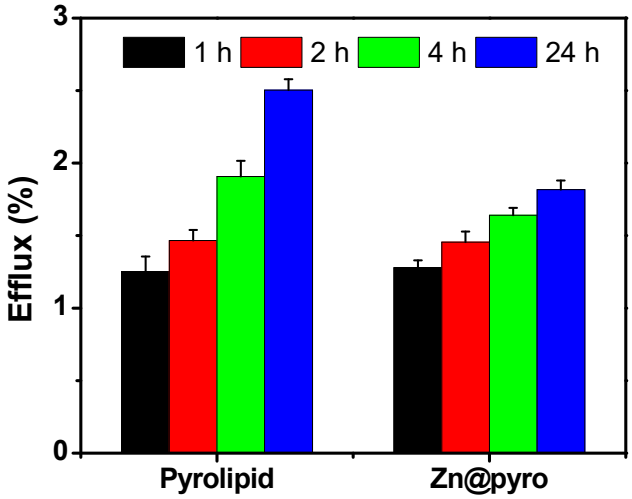

Figure S10. Efflux of free pyrolipid and ZnP@pyro by 4T1 cells. Cells were first incubated with free pyrolipid and ZnP@pyro for 4 h, then the culture medium was replaced by fresh medium and further incubated for 1, 2, 4, and 24 h. The pyrolipid amounts detected in the culture medium were compared with the 4-h uptake amounts to give the percent efflux.

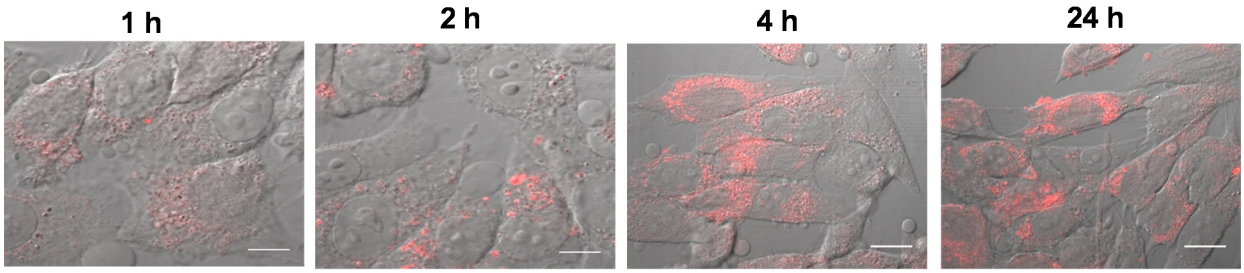

Figure S11. Confocal imaging showing the time-dependent cellular uptake of ZnP@pyro in 4T1 cells (scale bar = 20 μm).

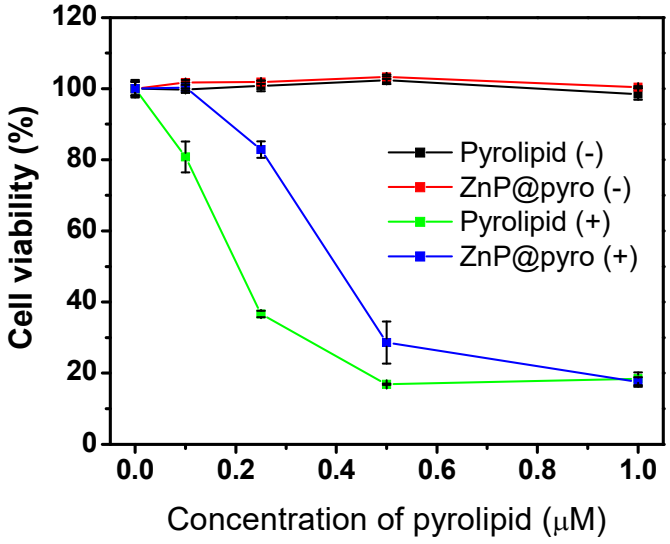

Figure S12. Cell viability of 4T1 cells treated with ZnP@pyro at different pyrolipid concentration. (+) and (-) in the legend represent cells with or without 15-min irradiation at 60 mW/cm^2.

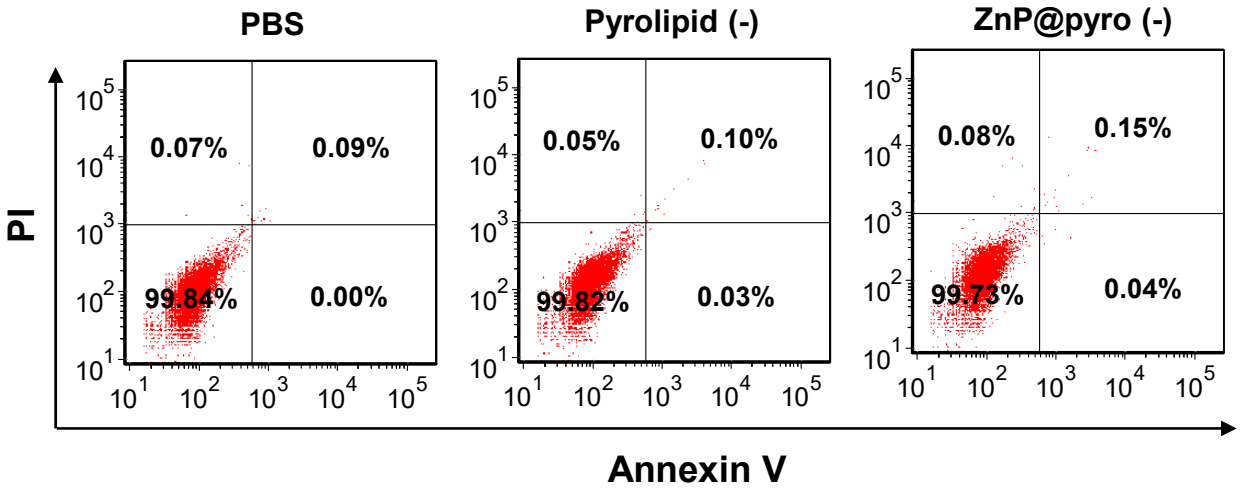

Figure S13. Apoptosis and/or necrosis of 4T1 tumor cells treated with ZnP@pyro without light irradiation by flow cytometry analysis. "(-)" in the figure legends refer to treatments without irradiation.

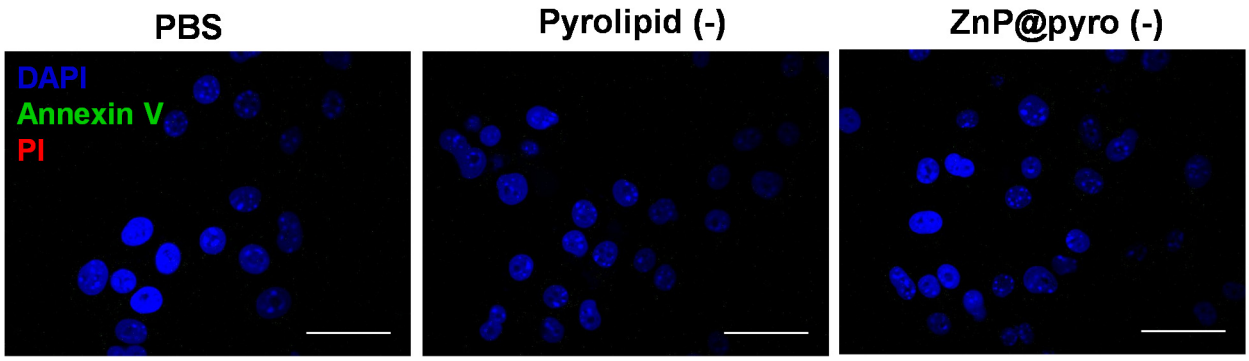

Figure S14. Confocal imaging showing no apoptosis and/or necrosis of 4T1 tumor cells were induced by free pyrolipid and ZnP@pyro without light irradiation. "(-)" in the figure legends refer to treatments without irradiation (scale bar = 50 μm).

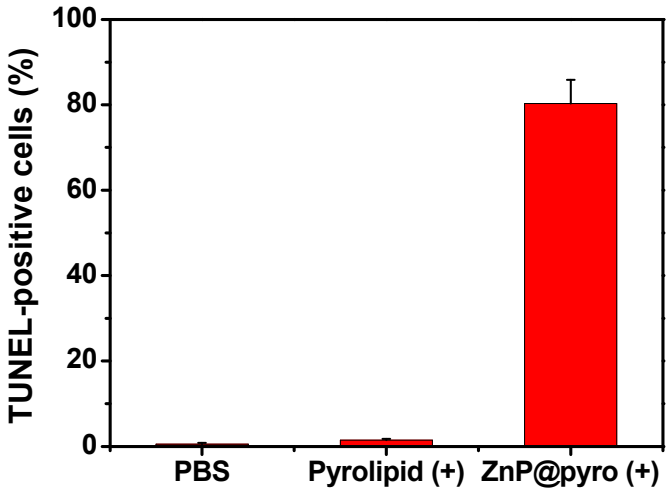

Figure S15. The percentage of TUNEL-positive cells in tumor tissues treated with pyrolipid or ZnP@pyro PDT.

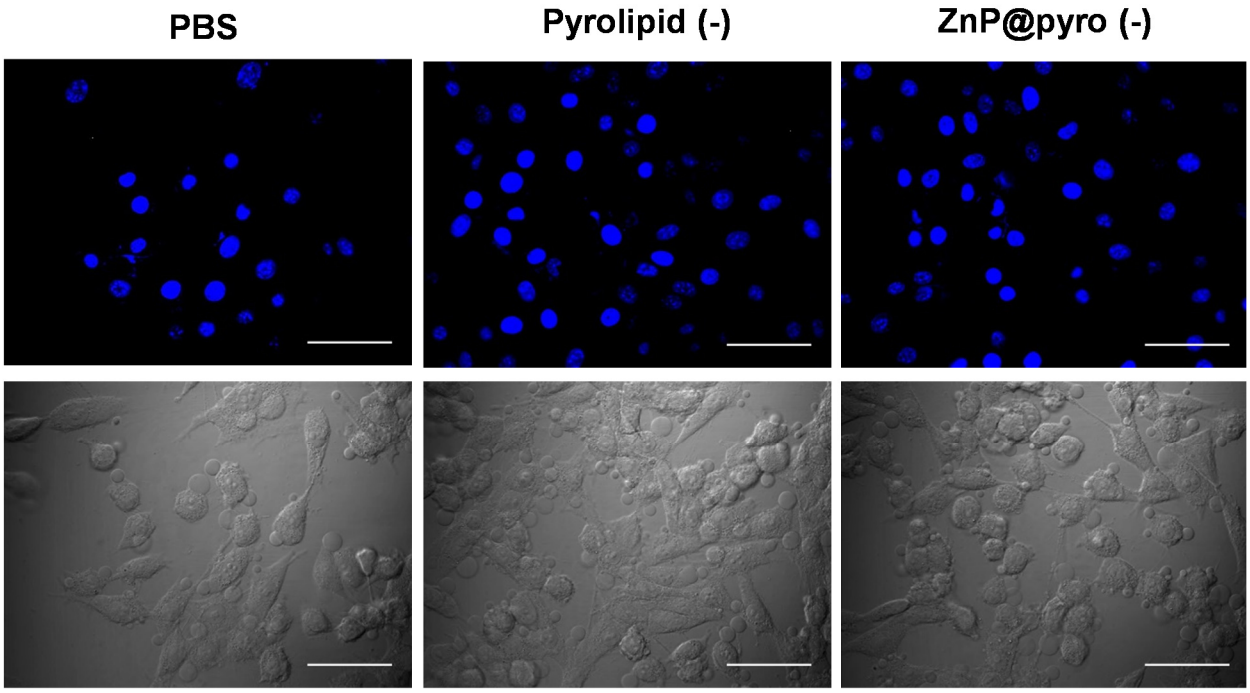

Figure S16. Immunofluorescence microscopy of CRT expression on the surface of 4T1 cells treated with PBS, free pyrolipid and ZnP@pyro in the absence of light irradiation. Blue: DAPI stained nuclei; Green: Alexa Fluor 488-CRT antibody (scale bar = 50 μm).

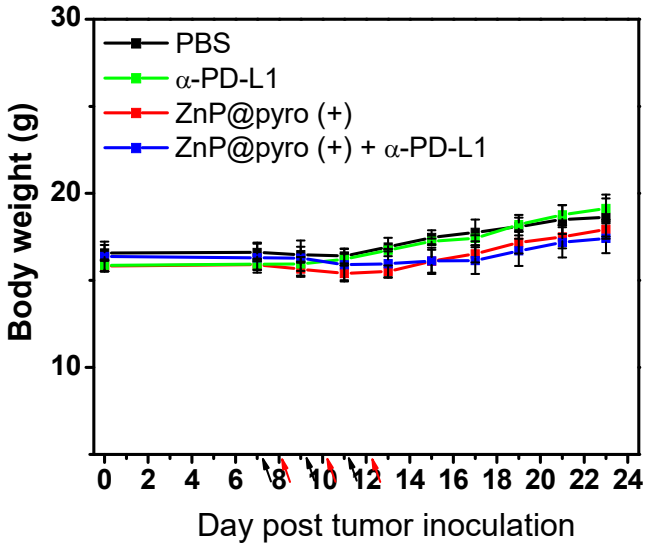

Figure S17. Body weight of 4T1 tumor-bearing mice receiving different treatments.

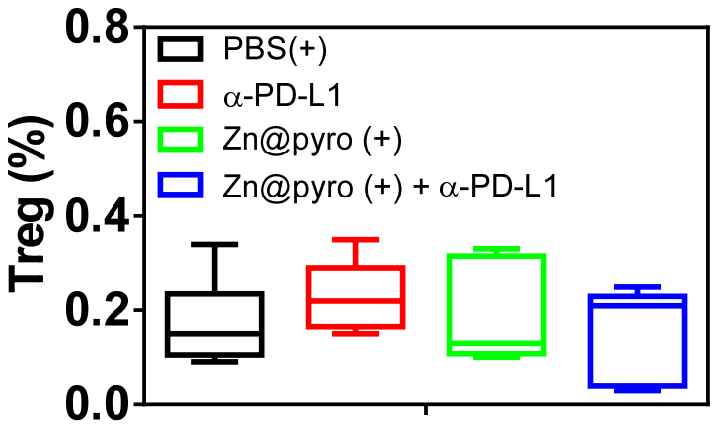

Figure S18. The percentages of Treg ($CD45^+CD4^+CD3e^+CD25^+Foxp3^+$) in total tumor cells, determined by flow cytometry.

Supporting Tables

Table S1. Summary of EXAFS fitting parameters for ZnP@pyro

Sample	ZnP@pyro
Fitting range	*k* 2.9 – 12.9 Å^{-1} *R* 1.0 – 3.45 Å
Independent points	15
Variables	8
Reduced chi-square	675.79
R-factor	0.006
S_0^2	1.000
ΔE_0(eV)	0.50±1.42
N (Zn-O)	4
***R* (Zn-O) (Å)**	1.965 ± 0.028
σ^2 (Zn-O) (Å^2)	0.007±0.002
N (Zn-P1)	0.48 ± 0.36
***R* (Zn-P1) (Å)**	2.896 ± 0.080
N (Zn-P1)	3.04 ± 0.72
***R* (Zn-P1) (Å)**	3.129 ± 0.019
σ^2 (Zn-P) (Å^2)	0.013±0.003

Table S2. IC_{50} values (μM) of free pyrolipid and ZnP@pyro with or without irradiation in 4T1 cells. Data are expressed as means ± s.d. (n = 3).

	60 mW/cm^2 15 min (54 J/cm^2)	Dark
Pyrolipid	0.22 ±0.01	> 5
Zn@pyro	0.42 ± 0.02	> 5

Supporting References

(1) Lovell, J. F.; Jin, C. S.; Huynh, E.; Jin, H.; Kim, C.; Rubinstein, J. L.; Chan, W. C.; Cao, W.; Wang, L. V.; Zheng, G. *Nat. Mater.* **2011,** *10*, 324.

(2) Rehr, J. J.; Albers, R. C. *Rev. Mod. Phys.* **2000,** *72*, 621.

(3) Ravel, B.; Newville, M. *J. Synchrotron Rad.* **2005,** *12*, 537.